

## Bandgap engineering of the perovskite materials for solar cell applications

<sup>1</sup>R. K. Shukla, <sup>2</sup>Amrit Kumar Mishra and <sup>3</sup>Susheel Kumar Singh

<sup>1</sup>Department of Physics, University of Lucknow, Lucknow - 226007, U.P. (India)

<sup>2</sup>Department of Physics, University of Lucknow, Lucknow - 226007, U.P. (India)

<sup>3</sup>Department of Physics, HLYB P.G. College Lucknow U. P. (India)

E-mail: rajeshkumarshukla\_100@yahoo.co.in

### Abstract:

Nowadays, Perovskite materials are frequently used in the application of solar cells. We are using organic-inorganic halide like  $\text{CH}_3\text{NH}_3\text{PbI}_3$ ,  $\text{CH}_3\text{NH}_3\text{PbCl}_3$  and  $\text{CH}_3\text{NH}_3\text{PbBr}_3$  in which  $\text{CH}_3\text{NH}_3$  is organic part, Pb is the inorganic part and I, Cl, Br is the halide atom. In all types of solar cells, I have worked on the perovskite solar cell nowadays which is frequently used in the energy harvesting materials for Solar cell applications. The perovskite solar cells have a rapid enhancement in the power conversion efficiency from 3.8% in 2009 to 23% in 2020. The good efficiency, large diffusion length, good photon absorption capacity, good mobility, low cost, and easy fabrication process motivated me to research perovskite solar cells. Photovoltaic systems combined with tandem solar cells have been successfully investigated to generate high power conversion efficiencies. Nevertheless, this fascinating concept has not yet been adequately applied to solar cells based on perovskite. In this chapter, we assess the feasibility of using perovskite semiconductors with different bandgaps for tandem concentric solar cell applications in combination with different bandgap for tandem concentric solar cell applications in combination with conventional crystalline silicon. We evaluate the device performance of tandem perovskite concentrator solar cells.

**Keywords:** perovskite, diffusion length, band gap, efficiency.

### 1. Introduction:

Nowadays, perovskite material is frequently used in solar cell devices as an active layer. The crystal structure of perovskite material  $\text{ABO}_3$ , A stands for an organic part ( $\text{CH}_3\text{NH}_3$ ), B stands for the inorganic part (Pb) of the material, and O stands for the halide atom (like Cl, Br, I) terminology used in the perovskite ( $\text{CH}_3\text{NH}_3\text{PbI}_3$ ) photovoltaic material. The phase transitions occur in the perovskite ( $\text{CH}_3\text{NH}_3\text{PbI}_3$ ) at 160 K from orthorhombic structure to tetragonal structure and at 327 K tetragonal to cubic structure obtain [1]. The  $\text{ABO}_3$  crystal structure of the Perovskite materials is shown in figure 1.

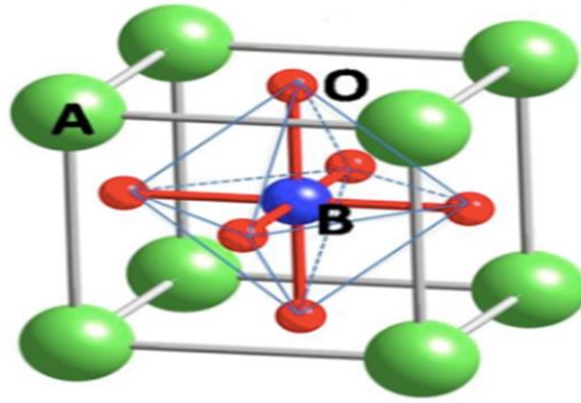


**Figure 1: The  $ABO_3$  crystal structure of the Perovskite materials**

The extraordinary material properties of the perovskite solar cell have a major role for the frequently used perovskite material in the device physics; The perovskite material has a long charge carrier diffusion length, high absorption coefficient, low exciton binding energy, and tuneable band gap [2-7]. However, Lab-scale device efficiency is higher than the commercially available solar cells, The stability issue exists in the perovskite solar cells since perovskite solar cell degradation concerning time, and degradation occurs due to air, UV light exposure, thermal stress (heat). light soaking, electric fields, humidity, and many other factors [8-10].due to this factor, we could not achieve the market requirement. Hence, we focused on the detailed degradation study of the perovskite solar cell for the improvement of device stability. The stability enhancement is done by adding UV filters, device encapsulation, and suppressing trap states (degradation caused by air and humidity), UV light, and electric fields, respectively [11-14]. During the operation of the perovskite solar cell thermal stress degradation occurs due to this, we will first focus on the structural change of perovskite material with a temperature change of the device. The device consists of many layers and this study specifically highlights the intrinsic degradation mechanisms of the perovskite absorber layer, including chemical, optical and morphological degradation.

## **2. Device Fabrication**

The solar cell fabrication technique was done by a spin coating method which is shown in Figures 2(a), 2(b), 2(c), and figure 3.

We are using patterned fluorine-doped tin oxide substrates (FTO) etched by Zn metal powder and dilute hydrochloric acid. The cleaning of etched FTO was done by sequential sonication technique into the soap solution, deionized water, and isopropanol for 15 min each. And next,

coat  $\text{TiO}_2$  (hole blocking layer) on it by using the spin coating method with 5000 rpm for 45 sec and heated at  $450^\circ\text{C}$  for 25 minutes, which is prepared by the mixture of 0.5 ml Ti (IV) isopropoxide (Sigma Aldrich), 7.25 ml of ethanol and 75 microliters of concentrated HCl. A  $\text{TiO}_2$  Mesoporous layer is made by using a dilute solution of Dyesol 18 N-RT paste (1:3.5 w/w in ethanol) at 4000 rpm for 30 seconds and heated at  $500^\circ\text{C}$  for 30 minutes and the film thickness to be formed 360 nm.

### 2.1 Preparation of perovskite:

For the perovskite deposition,  $\text{TiO}_2$  films were transferred into the glove box. The perovskite layer was deposited.

### 2.2 $\text{TiCl}_4$ Treatment:

First, we take 2M  $\text{TiCl}_4$  (1 ml) in 100ml D.I. water and put  $\text{TiO}_2$  film's into the solution, and heat at  $80^\circ\text{C}$  in the oven. After that, the film is washed with water, ethanol, and dried with Ar gas, and then heated at  $500^\circ\text{C}$  for 30 minutes and again we take 1M  $\text{PbI}_2$  (462 mg) solution in DMF (1 ml) and stirring at  $40^\circ\text{C}$  up to dissolve, after that spin-coated at 6000 rpm for 5 sec. Heated for 25 min at  $70^\circ\text{C}$  on a hot plate, drop into MAI (8mg/ml) in isopropanol after that dip the  $\text{PbI}_2$  film into the above solution for 15 min, and then washed with isopropanol and then heated at  $70^\circ\text{C}$  for 15 min.

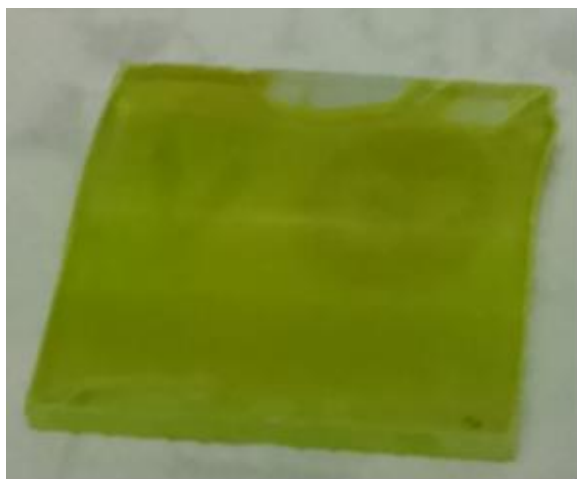


**Figure 2(a):  $\text{PbI}_2$  layer deposition on the FTO glass; (b):  $\text{CH}_3\text{NH}_3\text{PbI}_3$  layer deposition on FTO glass.**

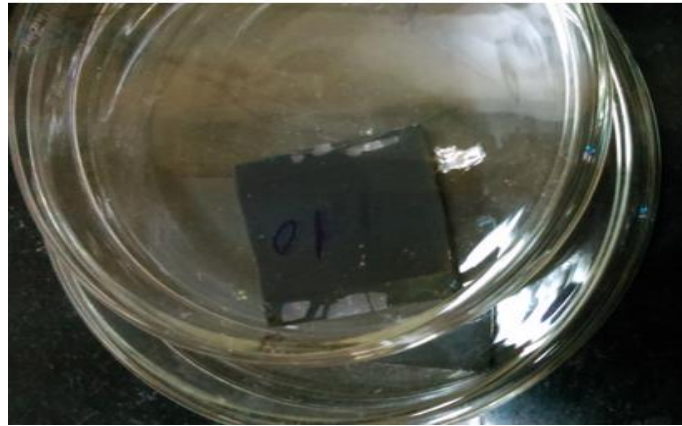


**Figure 2(c): perovskite film in the desiccator**

### **2.3 Spiro-MeOTAD Layer Deposition:**

First, we take 100 mL of Spiro-MeOTAD in 1 mL chlorobenzene 28.5 microliters of TBP (Tursary butyl pyridine) + Li salt solution (17.5 microliters) using spin coater at 4000 rpm for 30 sec and finally gold deposition on Spiro-MeOTAD layer by the thermal evaporator.

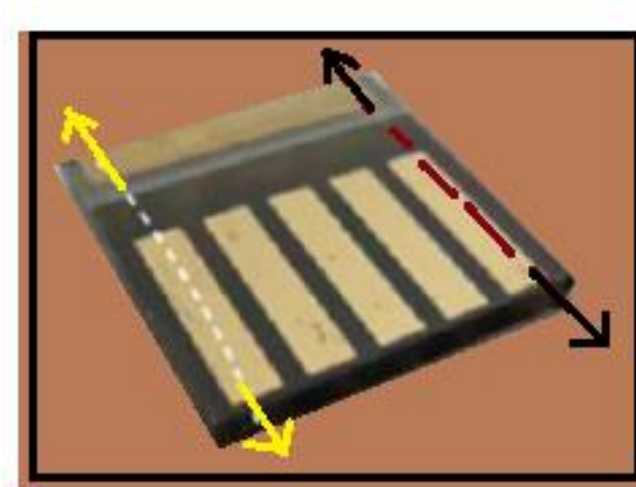


**Figure 3: The perovskite solar cell (the region under the Arrow showed the active area of the device)**

### **3.0 Electrical characterization of the perovskite solar cell:**

- J-V Characteristics
- C-V Characteristics
- C-f Characteristics
- I-Rh (%), Current – Relative humidity spectra.
- I-t, Current – Time spectra

- Noise spectroscopy

### **3.1 J-V Characteristics**

J-V measurements of the perovskite solar cell done by using Keithley 2450 source - measure unit under the AM1.5G 100 mW/cm<sup>2</sup> solar spectrum and light intensity measured by PM - 100 A compact power meter. The applied potential across the DUT (device under test) was +5 V to -5 V and the scan rate was 200 mV/s.

### **3.2 C-V Characteristics**

The apparatus used for the capacitance-voltage measurements of the perovskite solar cell were 4 MHz DSP Lock-in amplifier, Stanford Research System SR 865 A, and key sight 33621 A waveform generator.

### **3.3 C - f Characteristics**

The C - f measurements of the perovskite solar cell by using the SR 865 A, SR 560 voltage pre-amplifier, 4 MHz DSP Lock-in amplifier, and 33621 A waveform generator.

### **3.4 Current - Relative humidity I-Rh (%), Curve**

The electrical current versus relative humidity spectrum was observed in the perovskite solar cell by applied +5 V to -5 V DC source to the DUT (device under test) by Keithley 2450 source - measure unit under the AM1.5G 100 mW/cm<sup>2</sup> solar spectrum. Humidity control is done by sending wet nitrogen, dry nitrogen, humid air, or dry airflow to the humidity control chamber.

### **3.5 I-t, Current -Time spectra**

The electrical current versus time spectrum was observed at a fixed humidity level in the perovskite solar cell by applied +5 V to -5 V DC source to the DUT (device under test) by Keithley 2450 source - measure unit under the AM1.5G 100 mW/cm<sup>2</sup> solar spectrum.

### **3.6 Noise spectroscopy**

The study of noise allows the explanation of the electrical parameters of the defect states, charge carrier dynamics which are the major factors to explain the quality of the heterojunction solar cells and photovoltaic modules [4-5]. 1/f noise spectrum observed in the typical perovskite solar cells which are a powerful tool to the explanations of charge carriers injection, mobility of the photovoltaic material, defect states, and how 1/f noise spectrum shift after degradation of the perovskite solar cells. 1/f noise is the dominant noise in the Low-Frequency range and its spectral density is proportional to 1/f. Low-frequency 1/f noise is used to the model fluctuation of the device parameter with time.

## **4.0 Structural, Morphological and simulation of the perovskite solar cell**

#### 4.1 X-Ray diffraction

In the field of material science, condensed matter physics XRD investigation is a very important tool for the understanding of the crystal structure of bulk solids, thin films including lattice constant, the orientation of polycrystalline films, geometry, identification of unknown materials, defects, stress, determination of the particle size, etc. The electrons, neutrons are also used for diffraction studies from materials.

Mathematically, Bragg's law is bellowed.

$$2d\sin\theta = n\lambda$$

Where  $d$  is the inter planer spacing of the atoms,  $n$  is the order of diffraction,  $\lambda$  is the wavelength of light used during the XRD investigation and  $\theta$  is the glancing angle of X-rays. The pattern can then be compared with JCPDS (Joint committee on power diffraction standards) database cards or any other reported research work. Thus identification of given by Figure 4.

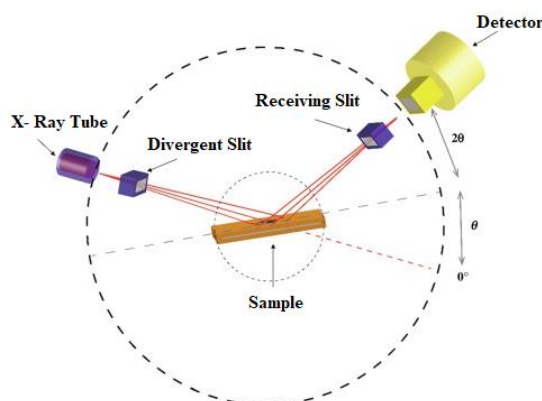


**Figure 4: The schematic diagram of the X-Ray Diffractometer**

#### 4.2 Scanning electron microscope (SEM)

The application of SEM is explored in the field of material science for the understanding of the surface morphology of the sample. The SEM is a type of electron microscope in which an image of a sample is taken by scanning the surface of the sample with a focused beam of electrons. The interaction of electrons with atoms in the sample creates various signals that contain information about the surface morphology, composition of the sample, and other properties such as electrical conductivity. The scanned electron beam develops a pattern, and

the position of the beam is combined with the intensity of the detected signal to produce an image.

SEM of the transverse cross-section of a homogeneous sample can indicate the thickness of the films. The most common or standard detection mode is secondary imaging where the scanning electron micrograph can produce a very high-resolution image of a sample surface revealing details about less than 1 nm in size. The very narrow electron beam facilitates a large depth of field yielding a characteristic three-dimensional appearance useful for understanding the surface structure of a sample. The schematic diagram of the image formation system of SEM is shown in Figure 10.

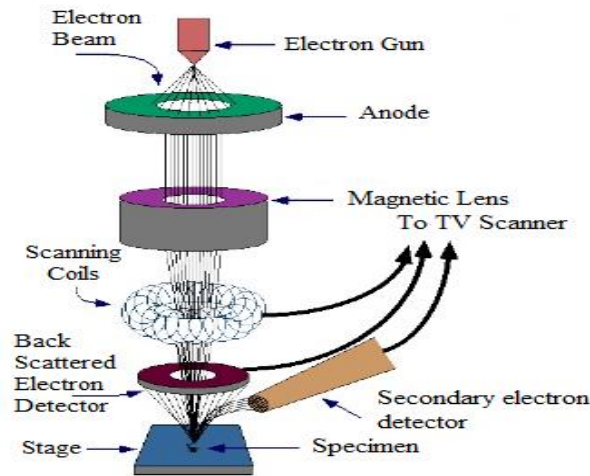


**Figure 10: The schematic diagram of the image formation system of SEM**

### Conclusion

We explained the basic physics of the solar cell and types of solar cell why perovskite is suitable for the energy harvesting material in the material science field and the history of the perovskite solar cell, bandgap engineering, and the different experimental characterization techniques for the explanation of the physical and chemical properties of the perovskite solar cell. Currently, crystalline silicon solar cells are dominant in the commercial and private PV market. The efficiency of these devices is high (>25%). However, these solar cells are thicker, heavier, and rigid when compared to thin-film PV technologies. Thin-film photovoltaics have already been implemented in the specific market such as extra-terrestrial solar panels. However, highly efficient (>25%) thin-film solar cells often use highly toxic or very expensive materials.

## Reference

- [1] Tanzila Tasnim Ava, Abdullah Al Mamun, Sylvain Marsillac and Gon Namkoong. A Review: Thermal Stability of Methylammonium Lead Halide Based Perovskite Solar Cells. *Appl. Sci.* **2019**, 9, 188; doi: 10.3390/app9010188.
- [2] Hao, F.; Stoumpos, C.C.; Cao, D.H.; Chang, R.P.; Kanatzidis, M.G. Lead-free solid-state organic–inorganic halide perovskite solar cells. *Nat. Photonics* **2014**, 8, 489. [CrossRef]
- [3] Lin, Q.; Armin, A.; Nagiri, R.C.R.; Burn, P.L.; Meredith, P. Electro-optics of perovskite solar cells. *Nat. Photonics* **2015**, 9, 106. [CrossRef]
- [4] Miyata, A.; Mitioglu, A.; Plochocka, P.; Portugall, O.; Wang, J.T.W.; Stranks, S.D.; Snaith, H.J.; Nicholas, R.J. Direct measurement of the exciton binding energy and effective masses for charge carriers in organic-inorganic tri-halide perovskites. *Nat. Phys.* **2015**, 11, 582–587. [CrossRef]
- [5] Stranks, S.D.; Eperon, G.E.; Grancini, G.; Menelaou, C.; Alcocer, M.J.; Leijtens, T.; Herz, L.M.; Petrozza, A.; Snaith, H.J. Electron-hole diffusion lengths exceeding 1 micrometer in an organometal trihalide perovskite absorber. *Science* **2013**, 342, 341–344. [CrossRef]
- [6] Xing, G.; Mathews, N.; Sun, S.; Lim, S.S.; Lam, Y.M.; Grätzel, M.; Mhaisalkar, S.; Sum, T.C. Long-range balanced electron-and hole-transport lengths in organic-inorganic CH<sub>3</sub>NH<sub>3</sub>PbI<sub>3</sub>. *Science* **2013**, 342, 344–347.[CrossRef]
- [7] Noh, J.H.; Im, S.H.; Heo, J.H.; Mandal, T.N.; Seok, S.I. Chemical management for colorful, efficient, and stable inorganic–organic hybrid nanostructured solar cells. *Nano Lett.* **2013**, 13, 1764–1769. [CrossRef] [PubMed]
- [8] Niu, G.; Guo, X.; Wang, L. Review of recent progress in chemical stability of perovskite solar cells. *J. Mater. Chem. A* **2015**, 3, 8970–8980. [CrossRef]
- [9] Grätzel, M. The light and shade of perovskite solar cells. *Nat. Mater.* **2014**, 13, 838. [CrossRef] [PubMed]
- [10] Li, X.; Tschumi, M.; Han, H.; Babkair, S.S.; Alzubaydi, R.A.; Ansari, A.A.; Habib, S.S.; Nazeeruddin, M.K.; Zakeeruddin, S.M.; Grätzel, M. Outdoor performance and stability under elevated temperatures and long-term light soaking of triple-layer mesoporous perovskite photovoltaics. *Energy Technol.* **2015**, 3, 551–555. [Cross Ref]

- [11] Han, Y.; Meyer, S.; Dkhissi, Y.; Weber, K.; Pringle, J.M.; Bach, U.; Spiccia, L.; Cheng, Y.B. Degradation observations of encapsulated planar CH<sub>3</sub>NH<sub>3</sub>PbI<sub>3</sub> perovskite solar cells at high temperatures and humidity. *J. Mater. Chem. A* **2015**, 3, 8139–8147. [Cross Ref]
- [12]. Leijtens, T.; Eperon, G.E.; Pathak, S.; Abate, A.; Lee, M.M.; Snaith, H.J. Overcoming ultraviolet light instability of sensitized TiO<sub>2</sub> with meso-superstructured organometal tri-halide perovskite solar cells. *Nat. Commun.* **2013**, 4, 2885. [Cross Ref]
- [13] Chen, W.; Wu, Y.; Yue, Y.; Liu, J.; Zhang, W.; Yang, X.; Chen, H.; Bi, E.; Ashraful, I.; Grätzel, M.; et al. Efficient and stable large-area perovskite solar cells with inorganic charge extraction layers. *Science* **2015**, aad1015.  
[CrossRef]
- [14] Shao, Y.; Yuan, Y.; Huang, J. Correlation of energy disorder and open-circuit voltage in hybrid perovskite solar cells. *Nat. Energy* **2016**, 1, 15001.